A Microfluidic Device With Optically-Controlled Electrodes for On-Demand Electrical Impedance Measurement of Targeted Single Cells

Na Liu, Ming Zhang, Tao Yue, Yuanyuan Liu, Yang Yang, Wen J. Li, *Fellow, IEEE*, and Yu Sun, *Fellow, IEEE*

***Abstract*— Electrical impedance measurement of a live cell is important for monitoring the cell's status. Label-free and non-invasive techniques for measuring the impedance of live cells have attracted much attention. Existing techniques are capable of measuring the impedance of entire cell populations and/or the instantaneous impedance of single cells, but an approach to track and monitor the electrical properties of single cells during their growth process has not yet been reported. This paper presents a microfluidic device integrated with optically-controlled electrodes (MOCE) for electrical impedance measurement of multiple individual cells over a time period. An equivalent circuit model to quantify the seal resistance, membrane capacitance, cytoplasmic resistance of single cells is proposed. In experiments, the adherence process of C2C12 myoblast cells was characterized by measuring individual cells' impedance data. During cell growth, the seal resistance R_{seal} increased gradually, while the membrane capacitance stayed at approximately 10^{-9} F and the cytoplasmic resistance stayed at approximately 10^{9} Ω. The results demonstrate the feasibility and effectiveness of the MOCE-based method for on-demand single-cell electrical impedance measurement. [2020-0265]**

***Index Terms*— Optically controlled electrode, microfluidic device, electrical impedance, single cell analysis, cell adherence.**

I. Introduction

THE electrical impedance of cells, as an important cellular property, is a useful label-free indicator of cell state and behaviour [1]. To understand the correlation between a cell's electrical properties and its states, techniques that are capable of monitoring the electrical impedance spectrum of single cells under different physiological conditions are demanded [2].

Several methods have been developed to characterize the electrical properties of cells, such as patch clamp, electrical cell substrate impedance sensing (ECIS), microfluidic impedance cytometry, and microelectrode array. Patch clamping has been used to study the processes of signal and synaptic transmission and to monitor intracellular and extracellular activity by suction of a cell with a micropipette under pulsed negative pressure [3], [4]. ECIS [1], [5], which measures the electrical impedance spectrum of cells through culturing cells on electrodes, is the most widely used method for investigating cellular events such as adhesion, proliferation, differentiation, and migration [6], [7]. It has been applied to cancer detection [8], [9], wound healing monitoring [10]–[12] and drug screen [13]–[15]. However, the traditional ECIS technique measures the entire cell population and does not target individual cells in the population. Microfluidic impedance cytometry takes advantage of hydromechanics as cells pass through a microchannel and records their electrical impedance spectrum individually [16]. This technique is suitable for detecting the instantaneous electrical impedance of a single cell but cannot track a specific cell over time. The combination of microfluidics and ECIS has also been demonstrated for the monitoring of a single cell [17]; however, it requires microchannels and microelectrodes to be fabricated with complicated structures. A device with prefabricated microelectrode arrays have also been used to measure the impedance spectrum of single cells by fabricating multiple microelectrodes and growing cells on the microelectrodes [18]. However, the tracking and measurement of only one cell is challenging with this technique.

This paper reports a microfluidic device with optically-controlled electrodes (MOCE) for on-demand monitoring of the electrical impedance of single cells. Virtual electrodes are dynamically generated on the substrate of the MOCE chip. Taking advantage of the virtual electrodes, the electrical impedance of any single cell on the substrate can be targeted and measured. The influence of parameters including channel height, light spot size and solution conductivity on impedance measurement have been discussed previously [19]. In this work, we propose a new circuit model to quantify the seal resistance, membrane capacitance, cytoplasmic resistance of single cells during 5-hour growth. The experimental results show that the seal resistance R_{seal} increased gradually, while the membrane capacitance and cytoplasmic resistance remained approximately unchanged during cell growth.

Manuscript received July 7, 2020; revised September 10, 2020; accepted September 21, 2020. Date of publication October 14, 2020; date of current version December 1, 2020. This research was supported in part by the National Natural Science Foundation of China (NSFC) under Grant 61703265, Grant 61933008, and Grant 61873307, and the Joint Fund of Science and Technology Department of Liaoning Province and State Key Laboratory of Robotics under Grant 2020-KF-22-07. Subject Editor C. Ahn. *(Corresponding authors: Na Liu; Yang Yang; Tao Yue.)*

Na Liu, Ming Zhang, Tao Yue, Yuanyuan Liu, and Yang Yang are with the School of Mechatronics Engineering and Automation, Shanghai University, Shanghai 200444, China (e-mail: liuna_sia@shu.edu.cn; tao_yue@shu.edu.cn; yangyang_shu@shu.edu.cn).

Wen J. Li is with the Department of Mechanical Engineering, City University of Hong Kong, Hong Kong (e-mail: wenjli@cityu.edu.hk).

Yu Sun is with the Department of Mechanical and Industrial Engineering, University of Toronto, Toronto, Canada (e-mail: sun@mie.utoronto.ca).

Color versions of one or more of the figures in this article are available online at https://ieeexplore.ieee.org.

Digital Object Identifier 10.1109/JMEMS.2020.3026726

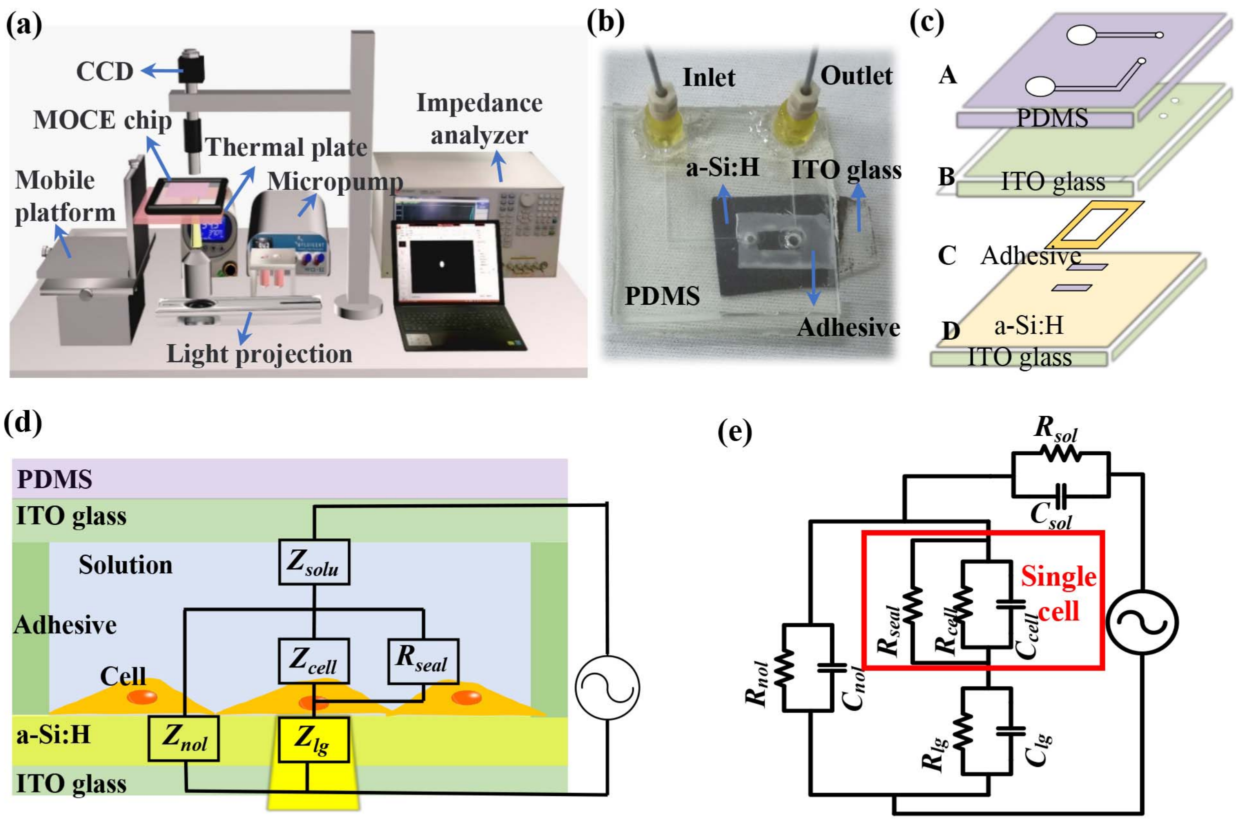

Fig. 1. (a) Illustration of the experimental system. (b) A photograph and (c) the labelled structure of the multi-layer MOCE chip. (d) Schematic diagram and (e) the equivalent circuit for characterizing the electrical properties of single cells in the MOCE chip.

II. Methods

A. Experimental Setup

The experimental system for on-demand measurement of the electrical impedance spectrum of single cells is shown in Fig. 1(a). The system is composed of seven modules, including an image acquisition module, a three-dimensional movable stage, an image projection system, a thermo plate, a micropump, an impedance analyser, and the MOCE device. As shown in Fig. 1(b)(c), the MOCE device consists of a polydimethylsiloxane (PDMS) layer with customised microfluidic channels for injecting cells and culture medium (Layer A), an upper ITO glass (Layer B), a double-sided adhesive tape (Layer C) patterned with a rectangular channel (length: 6 mm, width: 2 mm, height: 300 μm), and a photoconductive bottom substrate (Layer D), which is an ITO glass substrate coated with a hydrogenated amorphous silicon layer (a-Si:H) [20]. The PDMS channel layer was designed with two inlet holes (diameter: 0.8 mm) and two micro-channels (width: 0.8 mm, height: 0.5 mm) and was bonded with the upper ITO glass layer via oxygen plasma treatment. The microchannels on the PDMS layer were fabricated using the following steps. A PMMA template was first patterned by an engraving machine (Roland, EGX-350, Germany). The PDMS components were mixed with the curing agent at a ratio of 10:1 and were poured onto the PMMA template. The PDMS mixture was heated for 1.5 hour at 85°C and then peeled off for use. The upper ITO glass substrate was assembled with the bottom ITO glass substrate using the prefabricated double-sided adhesive. A PDMS film (length: 1 mm, W: 2 mm, H: 40 μm) was coated on both sides of the cell culture area to increase the impedance ratio of the light and dark hydrogenated amorphous silicon.

The image acquisition module includes a CCD camera (BASLER, ACA1300-30UC, Germany) attached to a microscope (Navitar, USA) for monitoring cell growth and for video acquisition. The image projection system is composed of a digital projector (Sony VPL-F600X, Japan), a condenser lens (Olympus, 50X, NA 0.50, WD 10.6 mm, Japan) and a computer used to generate and project an optical pattern onto the a-Si:H substrate. To measure the electrical impedance spectrum of single cells, a cell culture medium containing cells was injected into the micro-chamber between the upper ITO glass and the bottom a-Si:H substrate using a micropump (Fluigent, MFCS-EZ, France). The MOCE device was placed on a transparent thermal plate (Tokri Hit, Japan) used to maintain the appropriate temperature for cell culture. An impedance analyser (Keysight, E4990A, USA) was connected with the upper and bottom ITO substrates of the MOCE device to measure the electrical impedance of targeted cells on the a-Si:H substrate.

The a-Si:H film is a photoconductive layer whose conductivity increases from a dark conductivity of 10^{-9} S/m to a lighted conductivity of 10^{-4} S/m when illuminated by digitally projected patterns [21]. These projected light spots on the a-Si:H substrate function as dynamic "virtual" electrodes. The measurement of the electrical impedance spectrum of a single cell was realised by keeping the projected spot on the target cell.

B. Cell Preparation

Alcohol and PBS solution were injected into the chip to clean the MOCE device before injecting the cells. Next, mouse myoblast C2C12 cells (10^6 cells/mL) for technique testing were injected into the MOCE device and cultured in a mixture of high-glucose DMEM (HyClone) with 10% foetal bovine serum (Gibco) and 1% penicillin (Cellbio) at 37°C. HEPES buffer solution was added into this medium at a concentration of 20 mM/L to maintain PH value of the culture medium. A cell double-staining reagent (calcein-AM/PI) was used to indicate cell viability (with red for dead cells and green for living cells). The cell culture medium was injected into the MOCE device at a rate of 3.5 μl/min.

C. Equivalent Circuit Model

The equivalent circuit for calculating the electrical impedance of single cells using the MOCE device is shown in Fig. 1(d). Briefly, the equivalent circuit consists of four parts: (1) Z_{lg} and Z_{nol} represent the impedance of the a-Si:H substrate with light projection and without light projection, respectively; (2) Z_{cell} represents the impedance of measured single cells; (3) Z_{sol} represents the impedance of the cell culture medium; and (4) R_{seal} represents the sealing resistance, generated by the gap existing between the cell membrane and substrate [22]. The impedance of the interface between the culture medium and electrode substrate, referred to as Z_{ct} [19], was skipped in the present circuit model in order to extract the value of membrane capacitance, cytoplasmic resistance and seal resistance of single cells. Z_{ct} was neglected because Z_{ct} of the interface between the solution and a-Si:H without light projection was much lower than Z_{nol}. Z_{ct} of the interface between the solution and a-Si:H with light projection was included in the seal resistance of the cell. The impedance of the a-Si:H substrate with light projection, Z_{lg} is modelled by the resistance R_{lg} and capacitance C_{lg} in parallel. The impedance of the a-Si:H substrate without light projection, Z_{nol}, is modelled by the resistance R_{nol} and capacitance C_{nol} in parallel, as shown in Fig. 1(e). Single-cell impedance consists of cell membrane capacitance C_{cell} and cytoplasmic resistance R_{cell}. The impedance of the cell culture medium is modelled as the electrically parallel combination of the medium resistance R_{sol} and the capacitance C_{sol}. Due to the high conductivity of the cell culture medium, the capacitive reactance of the solution can be ignored [16]. The total impedance (Z_{total}) of the MOCE device can be expressed as

$$Z_{total} = \frac{Z_{cell} + \left(Z_{nol} + Z_{lg}\right) \times (R_{seal} + Z_{cell})}{Z_{nol} Z_{cell} + Z_{nol} Z_{lg} (R_{seal} + Z_{cell})} + Z_{sol} \quad (1)$$

where

$$z_{cell} = \frac{R_{cell}}{1 + j\omega C_{cell} R_{cell}} \quad (2)$$

$$z_{nol} = \frac{R_{nol}}{1 + j\omega C_{nol} R_{nol}} \quad (3)$$

$$z_{lg} = \frac{R_{lg}}{1 + j\omega C_{lg} R_{lg}} \quad (4)$$

$$z_{sol} = \frac{R_{sol}}{1 + j\omega C_{sol} R_{sol}} \quad (5)$$

The sealing resistance R_{seal} can be expressed as [23]

$$R_{seal} = \frac{\rho_s}{d}\delta \quad (6)$$

where ρ_s represents the resistivity of the solution, d represents the gap between the cell and the electrode, and δ represents the coincidence coefficient between the cell area and the electrode surface. R_{seal} is often used to indicate the adhesion degree between cells and their attached substrate.

D. Data Analysis

The parameters of the equivalent circuit were determined by a two-step procedure. First, the electrical impedance spectrum of the MOCE device without cells present was analysed using a reduced equivalent circuit by omitting the cell membrane capacitance C_{cell}, the cell cytoplasmic resistance R_{cell}, and any seal resistance R_{seal}. Afterwards, the electrical impedance spectrum of the MOCE device with cells was analysed with the entire equivalent circuit. The parameters for the electrical properties of single cells were determined by fitting the entire equivalent circuit with the ZView software (Scribner Associates, USA).

III. Results and Discussion

In the experiment, the conductivity of the culture medium was 1.67 S/m. The thickness of the chamber was 300 μm. A light spot with a constant diameter was applied to generate virtual electrode on a-Si:H substrate. Fig. 2(a) shows the light spot projected onto an adhered cell. To reduce the influence of the uneven density of hydrogenated amorphous silicon, the light spot was also projected onto a region without cells that was near the target adhered cell, as shown in Fig. 2(b). Fig. 2(c)-(d) shows the impedance of four different regions with single cell, and one region with no cell. The impedance spectrum when light spot was projected onto no cells was referred as $Impedance\_nocell$. The impedance when light spot was projected onto a single C2C12 cell was referred as $Impedance\_cell$. The frequency range of the measured impedance spectra was from 20 Hz to 10 MHz. As shown, all impedance magnitude decreased with increasing frequency.

The capacitive reactance decreased with increasing frequency, resulting in a decrease in the overall impedance. At low frequencies below 1 kHz, the value of $Impedance\_cell$ was slightly larger than the value of $Impedance\_nocell$, due to the cytoplasmic resistance R_{cell} and the seal resistance R_{seal}. However, at higher frequencies larger than 100 kHz, the value of $Impedance\_cell$ became much lower, because the

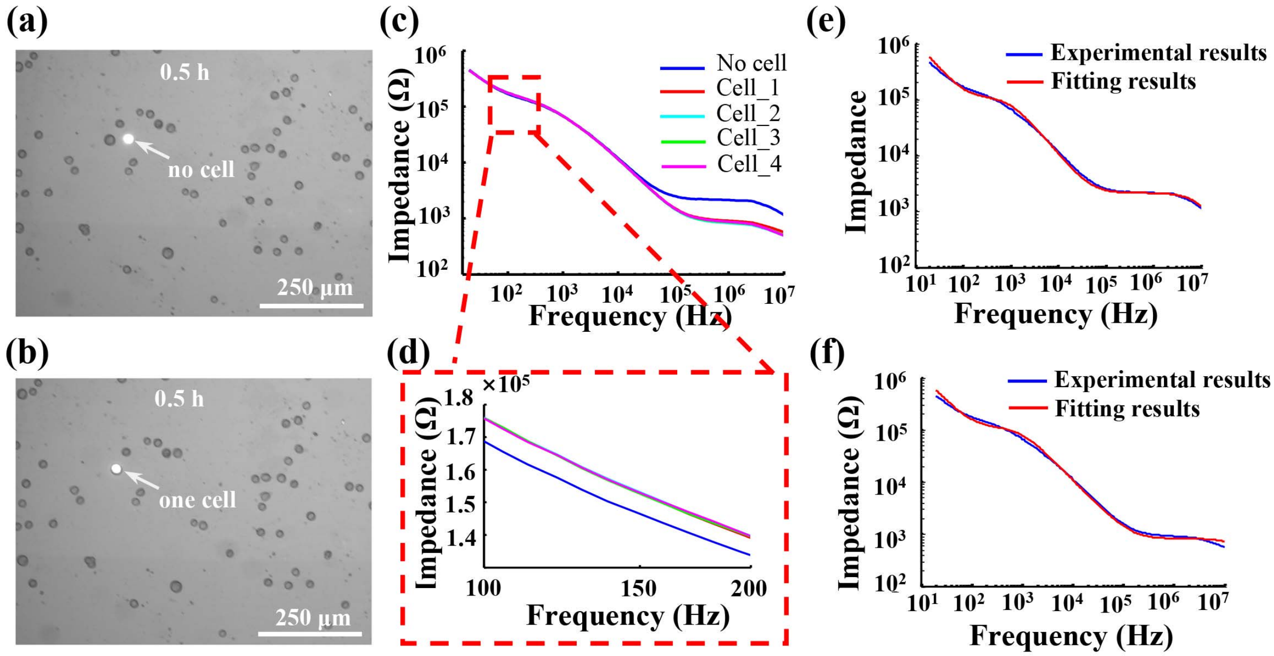

Fig. 2. (a) Light not projected on a cell. (b) Light projected on a C2C12 cell. (c) Impedance spectra when light was projected on no C2C12 cell and on one cell respectively. (d) Impedance spectra with frequency range of 100–200 Hz when light was projected on one C2C12 cell and on no cells, respectively. (e) The experimental and fitting results for $Impedance\_nocell$. (f) The experimental and fitting results for $Impedance\_cell$. $Note$: data were obtained at half an hour after injecting the cells into the MOCE chip.

impedance of the solution and of a single cell both decrease as frequency increase. In the high frequency case, the impedance of the solution and the cell membrane capacitance were the main factors affecting the overall impedance. Due to the difference between the impedance spectrum of $Impedance\_cell$ and $Impedance\_nocell$, the electrical properties of single C2C12 cells were determined.

The electrical properties of a cell were extracted by fitting the experimentally recorded impedance spectrum with the equivalent circuit model. Take the condition of one hour after injecting the cells into the MOCE device as an example for illustration. Fig. 2(e) shows the experimental and fitting results for the impedance spectrum of $Impedance\_nocell$. Fig. 2(f) shows the experimental and fitting results for the impedance spectrum of $Impedance\_cell$. The values of R_{lg}, C_{lg}, R_{nol} and C_{nol} were calculated based to the electrical properties of a-Si:H. Combined with these values, the impedance of the culture solution was determined through fitting the impedance spectrum of $Impedance\_nocell$. From the impedance of the culture medium and the a-Si:H, the cell membrane capacitance C_{cell}, cytoplasmic resistance R_{cell} and the seal resistance R_{seal} were extracted by fitting the impedance spectrum $Impedance\_cell$. For adhered C2C12 cells 5 hours after injection into the device, the value of membrane capacitance C_{cell} was determined to be $1.59 \pm 0.03 \times 10^{-9}$ F, the value of cytoplasmic resistance R_{cell} was $3.12 \pm 0.23 \times 10^{3}$ MΩ and the value of the seal resistance R_{seal} was about 1.08 ± 0.15 MΩ. Table I compares the quantified seal resistance and membrane capacitance of single cells measured by the MOCE and other techniques. As shown in Table I, the membrane capacitance values of different cell types quantified by different technique vary, and the seal resistance values all fall within the same order of magnitude.

TABLE I
MEASURED PARAMETERS OF SINGLE CELLS USING DIFFERENT TECHNIQUES

Cell Type	R_{seal} (MΩ)	C_{cell} (F)	Technique
C2C12	~1.08	1.59×10^{-9}	MOCE
NIH3T3	~1.69	−−	ECIS [24]
SkMel28	~1.00	$\sim 1.58 \times 10^{-12}$	FET [25]
HEK293	~1.31	$\sim 0.21 \times 10^{-13}$	ECIS-FET [26]
786-O	−−	$\sim 4.59 \times 10^{-11}$	MIC [27]
T2	−−	$\sim 5.66 \times 10^{-11}$	MIC [27]
Cardiacmyocyte	−−	$\sim 1.23 \times 10^{-10}$	Patch-clamp [28]

$Note$: Microfluidic device integrated with optically-controlled electrodes (MOCE), Electrical Cell substrate Impedance Sensing (ECIS), Field-Effect Transistors (FET) and Microfluidic Impedance Cytometry (MIC)

When cells grow on the substrate, cells take advantage of proteins (e.g., fibronectin) expressed on the cell surface to form adhesion with the substrate. These proteins also regulate the cytoskeleton through cellular signal transduction to spread the cell body [29]. The states of cell adhesion and spreading are important characteristics of cell growth.

Here, the cell adhesion state was characterized by monitoring the change in the seal resistance R_{seal} of the cell. Fig. 3 shows the state of the C2C12 cells injected into the MOCE device after 0.5, 1, 3 and 5 hours. As shown in Fig. 3(a), the C2C12 cells were largely spherical when they were initially injected into the MOCE device. The shapes of

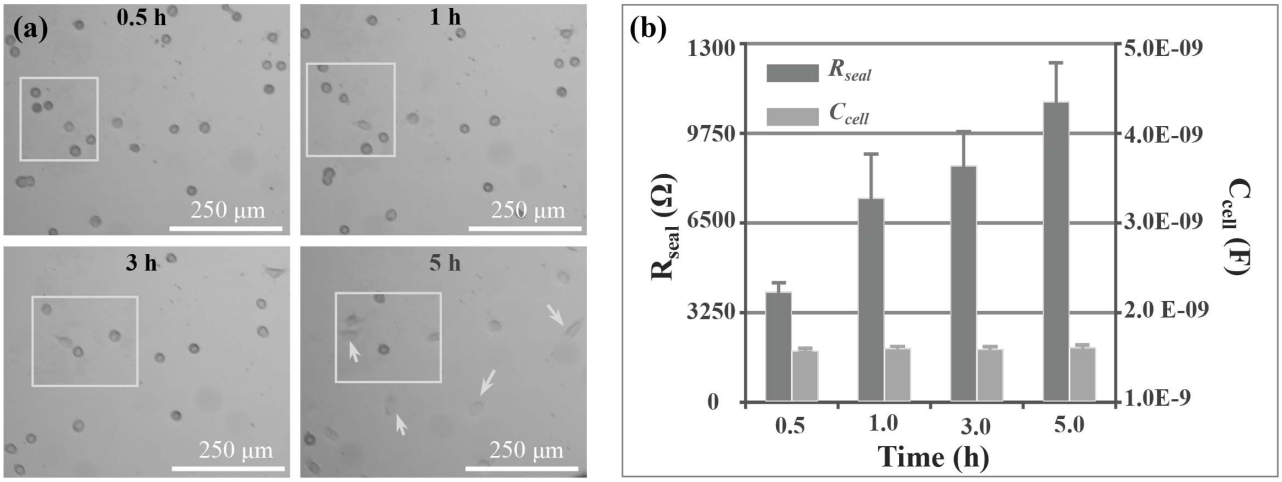

Fig. 3. (a) Images of cells 0.5, 1.0, 3.0 and 5.0 hours after injected into the MOCE device. (b) R_{seal} and C_{cell} values of the cells 0.5, 1.0, 3.0 and 5.0 hours after injected into the MOCE device. For each bar, 6 cells were measured.

the cells became flat after 1 hour, indicating that the cells started to attach to the substrate. After 5 hours, the cells were fully spreading on the substrate of the MOCE device, as pointed out by the white arrows. Fig. 3(b) shows changes in the sealing resistance R_{seal} of the single cells after 0.5, 1, 3 and 5 hours. The sealing resistance R_{seal} gradually increased from 0.37±0.04 MΩ at 0.5 h to 0.74±0.16 MΩ at 1.0 h to 0.86±0.13 MΩ at 3 h to 1.09±0.15 MΩ at 5 h as the cells adhered and spread on the MOCE device substrate, while the cell capacitance remained at approximately 10^{-9} F and the cytoplasmic resistance R_{cell} remained at a level of 10^9 Ω. The R_{seal} of single cells is an intrinsic electrical characteristic depending on the gap and the coincidence coefficient between the cell area and the electrode surface. Higher values for the R_{seal} represent tighter contact between the cell and the substrate [25], [26], [30]. Additionally, the cells after 5-hr measurements were stained using Calcein-AM/PI dye for cell viability analysis and the staining results suggested that the cells after 5-hr measurements were still viable.

IV. Conclusion

This paper reported a MOCE chip for characterising the electrical impedance of single cells in real time. An equivalent circuit model for extracting the impedance of single cells is presented. A cell within a population can be targeted on demand. The electrical impedance spectra of a single cell was monitored during its growth. The dynamic adherence behaviour of single C2C12 myoblast cells were revealed by the changes in seal resistance R_{seal} by fitting impedance spectra with the equivalent circuit for each time point. The electrical properties of cell including seal resistance, membrane capacitance and cytoplasmatic resistance are important parameters indicating cell attachment, apoptosis and other behaviors, which have potential applications in drug screening [24], [31]. Compared with traditional ECIS devices, the MOCE method can obtain the impedance of targeted single cells due to the flexible optically-controlled "virtual" electrodes. The flexibility of the MOCE method makes it suitable for single-cell monitoring and analysis. Next step research will involve the testing of multiple types of cells as well as their drug responses.

References

[1] I. Giaever and C. R. Keese, "Use of electric fields to monitor the dynamical aspect of cell behavior in tissue culture," *IEEE Trans. Biomed. Eng.*, vol. BME-33, no. 2, pp. 242–247, Feb. 1986.

[2] P. O. Bagnaninchi and N. Drummond, "Real-time label-free monitoring of adipose-derived stem cell differentiation with electric cell-substrate impedance sensing," *Proc. Nat. Acad. Sci. USA*, vol. 108, no. 16, pp. 6462–6467, Apr. 2011.

[3] O. P. Hamill, A. Marty, E. Neher, B. Sakmann, and F. J. Sigworth, "Improved patch-clamp techniques for high-resolution current recording from cells and cell-free membrane patches," *Pflügers Archiv-Eur. J. Physiol.*, vol. 391, no. 2, pp. 85–100, Aug. 1981.

[4] E. Neher and B. Sakmann, "Single-channel currents recorded from membrane of denervated frog muscle fibres," *Nature*, vol. 260, no. 5554, pp. 799–802, Apr. 1976.

[5] I. Giaever and C. R. Keese, "Monitoring fibroblast behavior in tissue culture with an applied electric field," *Proc. Nat. Acad. Sci. USA*, vol. 81, no. 12, pp. 3761–3764, Jun. 1984.

[6] J. Wegener, C. R. Keese, and I. Giaever, "Electric cell-substrate impedance sensing (ECIS) as a noninvasive means to monitor the kinetics of cell spreading to artificial surfaces," *Exp. Cell Res.*, vol. 259, no. 1, pp. 158–166, Aug. 2000.

[7] C. Xiao, B. Lachance, G. Sunahara, and J. H. T. Luong, "An in-depth analysis of electric cell-substrate impedance sensing to study the attachment and spreading of mammalian cells," *Anal. Chem.*, vol. 74, no. 6, pp. 1333–1339, Mar. 2002.

[8] A. R. A. Rahman, C.-M. Lo, and S. Bhansali, "A detailed model for high-frequency impedance characterization of ovarian cancer epithelial cell layer using ECIS electrodes," *IEEE Trans. Biomed. Eng.*, vol. 56, no. 2, pp. 485–492, Feb. 2009.

[9] J. Hong, K. Kandasamy, M. Marimuthu, C. S. Choi, and S. Kim, "Electrical cell-substrate impedance sensing as a non-invasive tool for cancer cell study," *Analyst*, vol. 136, no. 2, pp. 45–237, 2011.

[10] Y. Koo and Y. Yun, "Effects of polydeoxyribonucleotides (PDRN) on wound healing: Electric cell-substrate impedance sensing (ECIS)," *Mater. Sci. Eng., C*, vol. 69, pp. 554–560, Dec. 2016.

[11] C. R. Keese, J. Wegener, S. R. Walker, and I. Giaever, "Electrical wound-healing assay for cells *in vitro*," *Proc. Nat. Acad. Sci. USA*, vol. 101, no. 6, pp. 1554–1559, Feb. 2004.

[12] Y. Cui, Y. An, T. Jin, F. Zhang, and P. He, "Real-time monitoring of skin wound healing on nano-grooves topography using electric cell-substrate impedance sensing (ECIS)," *Sens. Actuators B, Chem.*, vol. 250, pp. 461–468, Oct. 2017.

[13] F. Xie, Y. Xu, L. Wang, K. Mitchelson, W. Xing, and J. Cheng, "Use of cellular electrical impedance sensing to assess *in vitro* cytotoxicity of anticancer drugs in a human kidney cell nephrotoxicity model," *Analyst*, vol. 137, no. 6, pp. 1343–1350, Mar. 2012.

[14] T. B. Tran, S. Cho, and J. Min, "Hydrogel-based diffusion chip with electric cell-substrate impedance sensing (ECIS) integration for cell viability assay and drug toxicity screening," *Biosensors Bioelectron.*, vol. 50, pp. 453–459, Dec. 2013.

[15] M. Parviz *et al.*, "Real-time bioimpedance sensing of antifibrotic drug action in primary human cells," *ACS Sensors*, vol. 2, no. 10, pp. 1482–1490, Oct. 2017.

[16] A. El Hasni, C. Schmitz, K. Bui-Göbbels, P. Bräunig, W. Jahnen-Dechent, and U. Schnakenberg, "Electrical impedance spectroscopy of single cells in hydrodynamic traps," *Sens. Actuators B, Chem.*, vol. 248, pp. 419–429, Sep. 2017.

[17] Y. Zhou, S. Basu, E. Laue, and A. A. Seshia, "Single cell studies of mouse embryonic stem cell (mESC) differentiation by electrical impedance measurements in a microfluidic device," *Biosensors Bioelectron.*, vol. 81, pp. 249–258, Jul. 2016.

[18] T. B. Tran, C. Baek, and J. Min, "Electric cell-substrate impedance sensing (ECIS) with microelectrode arrays for investigation of cancer cell—Fibroblasts interaction," *PLoS ONE*, vol. 11, no. 4, Apr. 2016, Art. no. e0153813.

[19] M. Zhang *et al.*, "A microfluidic-integrated optically-controlled electrodes chip for monitoring single cell's electrical impedance," in *Proc. IEEE 1st Int. Conf. Micro/Nano Sensors AI, Healthcare, Robot. (NSENS)*, Dec. 2018, pp. 15–19.

[20] N. Liu *et al.*, "Extracellular-controlled breast cancer cell formation and growth using non-UV patterned hydrogels via optically-induced electrokinetics," *Lab Chip*, vol. 14, no. 7, pp. 1367–1376, 2014.

[21] W. Liang, S. Wang, Y. Qu, Z. Dong, G.-B. Lee, and W. J. Li, "An equivalent electrical model for numerical analyses of ODEP manipulation," in *Proc. 6th IEEE Int. Conf. Nano/Micro Eng. Mol. Syst.*, Feb. 2011, pp. 825–830.

[22] Y. Xu, X. Xie, Y. Duan, L. Wang, Z. Cheng, and J. Cheng, "A review of impedance measurements of whole cells," *Biosensors Bioelectron.*, vol. 77, no. 77, pp. 824–836, 2016.

[23] T. Anh-Nguyen, B. Tiberius, U. Pliquett, and G. A. Urban, "An impedance biosensor for monitoring cancer cell attachment, spreading and drug-induced apoptosis," *Sens. Actuators A, Phys.*, vol. 241, pp. 231–237, Apr. 2016.

[24] F. Asphahani *et al.*, "Influence of cell adhesion and spreading on impedance characteristics of cell-based sensors," *Biosensors Bioelectron.*, vol. 23, no. 8, pp. 1307–1313, Mar. 2008.

[25] D. Koppenhöfer, A. Susloparova, J. K. Y. Law, X. T. Vu, and S. Ingebrandt, "Electronic monitoring of single cell-substrate adhesion events with quasi-planar field-effect transistors," *Sens. Actuators B, Chem.*, vol. 210, pp. 776–783, Apr. 2015.

[26] A. Susloparova, D. Koppenhöfer, J. K. Y. Law, X. T. Vu, and S. Ingebrandt, "Electrical cell-substrate impedance sensing with field-effect transistors is able to unravel cellular adhesion and detachment processes on a single cell level," *Lab Chip*, vol. 15, no. 3, pp. 668–679, 2015.

[27] Y. Zhao *et al.*, "A microfluidic system enabling continuous characterization of specific membrane capacitance and cytoplasm conductivity of single cells in suspension," *Biosensors Bioelectron.*, vol. 43, pp. 344–347, May 2013.

[28] M. Hoťka and I. Zahradník, "Reconstruction of membrane current by deconvolution and its application to membrane capacitance measurements in cardiac myocytes," *PLoS ONE*, vol. 12, no. 11, Nov. 2017, Art. no. e0188452.

[29] O. Chaudhuri *et al.*, "Substrate stress relaxation regulates cell spreading," *Nature Commun.*, vol. 6, no. 1, pp. 1–7, May 2015.

[30] A. Susloparova, X. T. Vu, D. Koppenhöfer, J. K.-Y. Law, and S. Ingebrandt, "Investigation of ISFET device parameters to optimize for impedimetric sensing of cellular adhesion," *Phys. Status Solidi A*, vol. 211, no. 6, pp. 1395–1403, Jun. 2014.

[31] F. Asphahani *et al.*, "Single-cell bioelectrical impedance platform for monitoring cellular response to drug treatment," *Phys. Biol.*, vol. 8, no. 1, p. 15006, 2011.

Na Liu received the B.S. degree in automation from Sichuan University, Chengdu, China, in 2010, and the Ph.D. degree from the State Key Laboratory of Robotics, Shenyang Institute of Automation, Chinese Academy of Sciences, Shenyang, China, in 2016. She is currently an Associate Professor with the School of Mechatronic Engineering and Automation, Shanghai University, Shanghai, China. Her research interests include micro- and nano-robotics, and their applications in bioengineering and biomedicine.

Ming Zhang received the M.S. degree in mechatronic engineering from Shanghai University in 2019. Her research interest includes micro- and nano-systems.

Tao Yue received the B.S. and M.S. degrees from Tongji University, Shanghai, China, in 2007 and 2010, respectively, and the Ph.D. degree from Nagoya University, Nagoya, Japan, in 2014. He is currently an Assistant Professor with the School of Mechatronic Engineering and Automation, Shanghai University, Shanghai, China. His research interests include micro/nano robotics and manipulation, single cell analysis, and micro/nano biotechnologies. He received the Best Paper Award at the IEEE International Symposium on Micro-Nano Mechatronics and Human Science in 2013, and the IEEE Robotics and Automation Society Japan Chapter Young Award in 2014.

Yuanyuan Liu received the B.S. and M.S. degrees in automation from the Shengyang University of Chemical Technology in 2004 and 2004, respectively, and the Ph.D. degree from Shanghai Jiao Tong University in 2008. She is currently a Professor with Shanghai University. Her research interests include in the area of bio-3D printing, bio-manufacturing, and micro-nano manipulation, and more research has been accumulated in the construction and active regulation of artificial biological tissues/organs.

Yang Yang received the Ph.D. degree from Ritsumeikan University, Kyoto, Japan, in 2015. From 2015 to 2016, he was a Post-Doctoral Researcher with the Department of Mechanical and Aerospace Engineering, Tokyo Institute of Technology, Tokyo, Japan. He is currently a Lecturer with the School of Mechatronic Engineering and Automation, Shanghai University, Shanghai, China. His research interests include soft robots, mobile robots, and terramechanics.

Wen J. Li (Fellow, IEEE) received the B.S. and M.S. degrees in aerospace engineering from the University of Southern California (USC), in 1987 and 1989, respectively, and the Ph.D. degree in aerospace engineering from the University of California at Los Angeles (UCLA), Los Angeles, CA, USA, in 1997. From 1997 to 2011, he was with the Department of Mechanical and Automation Engineering, The Chinese University of Hong Kong. His industrial experience includes the Aerospace Corporation, El Segundo, CA, USA, the NASA Jet Propulsion Laboratory, Pasadena, CA, USA, and Silicon Microstructures, Inc., Fremont, CA, USA. He is currently a Chair Professor with the Department of Mechanical and Biomedical Engineering, City University of Hong Kong. His current research interests include intelligent cyber physical sensors, super-resolution microscopy, and nanoscale sensing and manipulation. He served as the President of the IEEE Nanotechnology Council, in 2016 and 2017.

Yu Sun (Fellow, IEEE) received the bachelor's degree from the Dalian University of Technology, Dalian, China, in 1996, the first M.S. degree from the Institute of Automation, Chinese Academy of Sciences, Beijing, China, in 1999, and the second M.S. degree in electrical engineering and the Ph.D. degree in mechanical engineering from the University of Minnesota, Minneapolis, MN, USA, in 2001 and 2003, respectively, under the supervision of Prof. B. J. Nelson. He was a Post-Doctoral Researcher with the Swiss Federal Institute of Technology (ETH Zurich), Zürich, Switzerland. He joined the University of Toronto (UofT), Toronto, ON, Canada, in 2004, where he was promoted through the ranks of an Associate Professor and a Full Professor in 2009 and 2012, respectively. He is currently a Professor with the Department of Mechanical and Industrial Engineering and also jointly appointed with the Institute of Biomaterials and Biomedical Engineering and the Department of Electrical and Computer Engineering, a McLean Senior Faculty Fellow, and the Canada Research Chair of Micro and Nano Engineering Systems (Tier I). As the Faculty Director, he directed the University Nanofabrication Centre from 2012 to 2013. He was a recipient of the Alumni Achievement Award in 2015 from the Dalian University of Technology. In 2014, he was elected into the Canadian Academy of Engineering.